Inexpensive and fast pathogenic bacteria screening using field-effect transistors

Nello Formisano [a], Nikhil Bhalla [a], Mel Heeran [b], Juana Reyes Martinez [b], Amrita Sarkar [b], Maisem Laabei [c], Pawan Jolly [a], Chris R. Bowen [d], John T. Taylor [a], Sabine Flitsch [b], Pedro Estrela[a,*]

[a] Department of Electronic & Electrical Engineering, University of Bath, Bath BA2 7AY, United Kingdom. E-mails: n.f@hotmail.it (N.F.), nikhilbhalla151@gmail.com (N.B.), p.jolly@bath.ac.uk (P.J.), j.t.taylor@bath.ac.uk (J.T.T.), p.estrela@bath.ac.uk (P.E.)

[b] School of Chemistry & Manchester Institute of Biotechnology, The University of Manchester, Manchester M1 7DN, United Kingdom. E-mails: juana.reyesmartinez@manchester.ac.uk (J.R.M.), amrita.sarkar@manchester.ac.uk (A.S.), sabine.flitsch@manchester.ac.uk (S.F.)

[c] Department of Biology & Biochemistry, University of Bath, Bath BA2 7AY, United Kingdom. E-mail: maisemlaabei27@gmail.com (M.L.)

[d] Department of Mechanical Engineering, University of Bath, Bath BA2 7AY, United Kingdom. E-mail: c.r.bowen@bath.ac.uk (C.R.B.)

*Corresponding author: Department of Electronic & Electrical Engineering,
University of Bath,
Claverton Down, Bath, BA2 7AY, United Kingdom
E-mail: P.Estrela@bath.ac.uk
Phone: +44-1225-386324

Abstract

While pathogenic bacteria contribute to a large number of globally important diseases and infections, current clinical diagnosis is based on processes that often involve culturing which can be time-consuming. Therefore, innovative, simple, rapid and low-cost solutions to effectively reduce the burden of bacterial infections are urgently needed. Here we demonstrate a label-free sensor for fast bacterial detection based on metal–oxide–semiconductor field-effect transistors (MOSFETs). The electric charge of bacteria binding to the glycosylated gates of a MOSFET enables quantification in a straightforward manner. We

show that the limit of quantitation is 1.9×10^5 CFU/mL with this simple device, which is more than 10,000-times lower than is achieved with electrochemical impedance spectroscopy (EIS) and matrix-assisted laser desorption ionisation time-of-flight mass spectrometry (MALDI-ToF) on the same modified surfaces. Moreover, the measurements are extremely fast and the sensor can be mass produced at trivial cost as a tool for initial screening of pathogens.

Keywords: biosensors, BioFET, electrochemical impedance spectroscopy, MALDI-ToF, bacteria

1. Introduction

Bacterial infection has a profound impact on global health (Coates *et al.*, 2002) and contributes to globally important diseases, such as tuberculosis, pneumonia, tetanus, typhoid fever, diphtheria, syphilis, and is the cause of high infant mortality rates in developing countries; bacterial infection is also believed to be responsible for more than 20% of human tumours worldwide (Brachman & Abrutyn, 2009; Stein, 2011). The methods by which bacteria are currently detected in routine clinical microbiology involve processes consisting of an initial sample growth step where all the species in a sample are cultured in a rich medium in order to obtain a sufficient mass for a subsequent analysis. The post-growth analysis allows isolation and characterisation of single species in a sample, usually by means of techniques such as staining, real-time polymerase chain reaction (RT-PCR), whole genome sequencing (WGS) and matrix-assisted laser desorption ionisation time-of-flight mass spectrometry (MALDI-ToF MS) (see *e.g.* Fournier *et al.*, 2013 and references therein). Although elegant and effective alternative approaches to microorganism detection have been reported (Mannoor *et al.*, 2012; Zourob *et al.*, 2008; Ma *et al.*, 2015), where single bacteria sensing could be achieved (Kang *et al.*, 2014; Mohanty & Berry, 2008), the current 'gold standard' for clinicians is still represented by culturing methods, nucleic acid-based sensors, immunoassays and fluorescence-based techniques (Ahmed *et al.*, 2014). Limitations on the adoption of new solutions for diagnosis include the complexity of the fabrication of new sensors, the complexity of assay implementation and sample processing, and the prohibitive costs of introducing new equipment to perform bacterial detection. In order to overcome such obstacles while simultaneously introducing improvements in the current diagnostics, simple,

readily available sensors must be developed. The introduction of fast, simple and low-cost sensors that could be easily employed in clinical laboratories would dramatically reduce both the time and the cost of current bacterial diagnosis. For instance, a device that is able to provide an initial screening of a sample at the initial growth stage with adequate detection regarding its pathogenicity would be able to confirm the need to perform more complex and expensive analysis. Given the status of national health systems worldwide and the ever present need to reduce the cost of public healthcare, only very inexpensive, easily fabricated devices that are able to perform in a rapid manner and with parallel screening would be currently capable of supporting effectively clinical microbiology.

We here report on a label-free bacterial detection system using biologically-sensitive field-effect transistors (BioFETs) (Poghossian & Schöning, 2014). The BioFETs were constructed by immobilising a bioreceptor layer onto an extended gate of a metal–oxide–semiconductor field-effect transistor (MOSFET). MOSFETs are ubiquitous electronic components that can easily and cheaply be expanded into arrays for high-throughput screening. BioFETs with extended gold gates have previously been used for the detection of DNA hybridisation (Estrela *et al.*, 2005) and proteins (Estrela *et al.*, 2010). In this study we demonstrate the detection of mannose-specific type 1 fimbrial *Escherichia coli* PKL1162 as a case study for MOSFET-based bacterial detection.

Amongst pathogenic bacteria, uropathogenic *Escherichia coli* (UPEC) are responsible for urinary tract infections. UPEC is the most predominant uropathogen causing approximately 80% of uncomplicated infections (Ronald, 2003). It is estimated that between 40-50% of females and 15% of males will develop urinary infections and the rate of recurrent infections has been reported to be as high as 30% (Foxman *et al.*, 2000). In order to colonise the cells of the urinary conducts and trigger a disease, UPEC can exploit hair-like protein structures expressed on their surface (called fimbriae), which allow bacteria to firmly adhere on the cells' surface and not be washed away in the urinary flow. Lectin protein structures, that constitute fimbriae, are expressed in at least 9 out of 10 UPEC strains (Oelschlaeger *et al.*, 2002). As the specificity can vary towards different glycosylated surfaces, several carbohydrate-specific fimbriae have been found and, amongst them, mannose-specific type 1 fimbriae is classified as one of the most commonly expressed (Hartmann & Lindhorst, 2011). The recognition event interests the glycosylated cell of the urinary tract and the mannose-specific protein, called FimH, situated at the tip of the fimbrial rod of the pathogenic bacteria.

The electric charge of bacteria binding to the glycosylated gate of a MOSFET enables quantification in a straightforward manner. Both the charges on the membrane of the bacteria and the displacement of water and ions from the biolayer surface when a bacteria is present, disturbs significantly the electrochemical double layer capacitance, which causes a threshold potential shift on the BioFETs. Very low limits of detection can be obtained with the technique. As a comparison, the same electrodes were used for electrochemical impedance spectroscopy (EIS) and matrix-assisted laser desorption ionisation time-of-flight mass spectrometry (MALDI-ToF) – both techniques show significantly higher limits of detection than the BioFETs.

2. Materials and methods

2.1. Bacteria preparation

Uropathogenic *Escherichia coli* strain PKL1162 was obtained by engineering the strain SAR18 with the plasmid pPKL174 (Reisner *et al.*, 2003). The bacteria were grown overnight while shaking in an incubator at 37℃ in lysogen broth growing media. The bacteria were then harvested by centrifugation at 4000 rpm for 15 min at 4 °C. The pelleted bacterial cells were resuspended in 10 mL of PBS Buffer and harvested twice before a final resuspension in 1 mL of PBS Buffer for their quantification and use.

2.2. Electrode functionalisation and affinity capture assay

A mixture of HS-$(CH_2)_{17}$-$(OC_2H_4)_3$-OH and HS-$(CH_2)_{17}$-$(OC_2H_4)_6$-OCH_2COOH in a ratio 1:4 was used for the SAM formation. The mixture, obtained by mixing 53 µL of HS-$(CH_2)_{17}$-$(OC_2H_4)_6$-OCH_2COOH (0.476 mM, 0.2 mg/mL in DMSO) and 147 µL of HS-$(CH_2)_{17}$-$(OC_2H_4)_3$-OH (0.328 mM, 0.2 mg/mL in DMSO) was sonicated for 20 minutes and used for the overnight incubation with the electrodes at room temperature in a humidity chamber.

Aminoethyl glycosides in PBS at the concentration of 50 mM were immobilised overnight in humidity chamber at room temperature overnight after activation of the carboxyl groups using a solution of EDC/sulfo-NHS at the concentration of 40 mM and 10 mM, respectively, for 1 hour. Once the glycosides were immobilised, a blocking step of the non-reacted sites was performed using a 10 mM ethanolamine aqueous solution at pH 8.5 for 20 minutes. The bacteria affinity capture was performed by incubating the electrodes at 37 °C for 1.5 hours.

Immobilised α-D-mannose was used to affinity capture uropathogenic *Escherichia coli* strain PKL1162 while 2-Acetamido-2-deoxy-α-D-galactopyranose (GalNAc) was used as a control glycan. A further control was performed by measuring the interaction between α-D-mannose and the *Escherichia coli* strain K12.

The assay was carried out on in-house fabricated arrays of gold electrodes (100 nm thickness deposited on 20 nm of chromium on glass substrates by means of thermal evaporation through a shadow mask).

2.3. Measurements set up

The extended-gate FET sensor with gold thin film electrode consisted of two parts: (i) an array of gold electrodes, where bacteria were captured, and (ii) the FET structure, which transduces the binding events on the gold electrode into electrical signals. The extended gate was fabricated by connecting the Au electrodes, fixed in a reaction cell, to the gate of a MOSFET *via* a metal wire.

The BioFET measurements were carried out connecting the in-house fabricated arrays of gold electrodes to the gate of an n-type MOSFET. The MOSFET readings were taken using an Agilent B1500A HR CMU Semiconductor Device Analyser.

The bacterial detection is initially demonstrated by performing electrochemical impedance spectroscopy (EIS) capacitive measurements. The capacitance (C) indicates the capacity of a material to store charge (Q) due to a potential difference (V) and is given by the expression $C = \frac{Q}{V}$, which, for a parallel plate capacitor, can be rewritten as $C = \frac{\varepsilon_o \varepsilon_r A}{d}$, where ε_o is the permittivity of the vacuum, ε_r is the relative permittivity that depends on the material between the two plates having a surface area A that are a distance d from each other. The imaginary and real part of the complex capacitance (C' and C'' respectively) were calculated from the measured impedance using equation (1) (Formisano *et al.*, 2015):

$$C^* = C' + jC'' = \frac{1}{j\omega Z} \qquad (1)$$

The percentage change of capacitance from each step where then calculated considering only the real part of the capacitance, C', at the frequency where the absolute value of the imaginary value, C'', has its relative minimum. This frequency was 10 Hz throughout the experiments.

For the EIS recordings, non-Faradaic measurements were carried out in a phosphate buffer saline (PBS) solution diluted 100 times (ionic strength equal to 1.62 mM) without redox markers. The same measurement solution conditions were applied for MOSFET readings.

EIS measurements were taken in a three electrode system using an Ag/AgCl as reference electrode and applying a 10 mV AC signal superimposed to 0 mV DC bias voltage *vs.* the open circuit potential.

The same electrodes were analysed by MALDI-ToF mass spectrometry. Since large area electrically conducting surfaces are needed for MALDI-ToF measurements, the back of the glass slides used for EIS and BioFET measurements were covered with silver paint or with a conductive aluminium tape (Weissenborn *et al.*, 2012). In addition, gold MALDI plates (AB Sciex Ltd) were used as a platform containing self-assembled biorepulsive monolayers of functionalised alkanethiols to which several aminoethyl glycosides were covalently attached (Šardzík, R. *et al.*, 2010) to alternatively compare measurements obtained from the BioFETs.

3. Results and discussion

In our work, specific glycan interactions were studied on electrodes modified with self-assembled monolayers (SAMs). The functionalised electrodes were connected to the gates of n-channel enhancement MOSFET devices, hence generating BioFETs (Figure 1). Mannosides were immobilised on the electrodes and used to affinity capture uropathogeninc *Escherichia coli* strain PKL1162 (Reisner *et al.*, 2003). The surface chemistry was previously optimised and monitored by MALDI-ToF to obtain maximum bacteria binding (Both *et al.*, 2014; Noble *et al.*; 2012; Šardzik *et al.*, 2012; Zhi *et al.*, 2008).

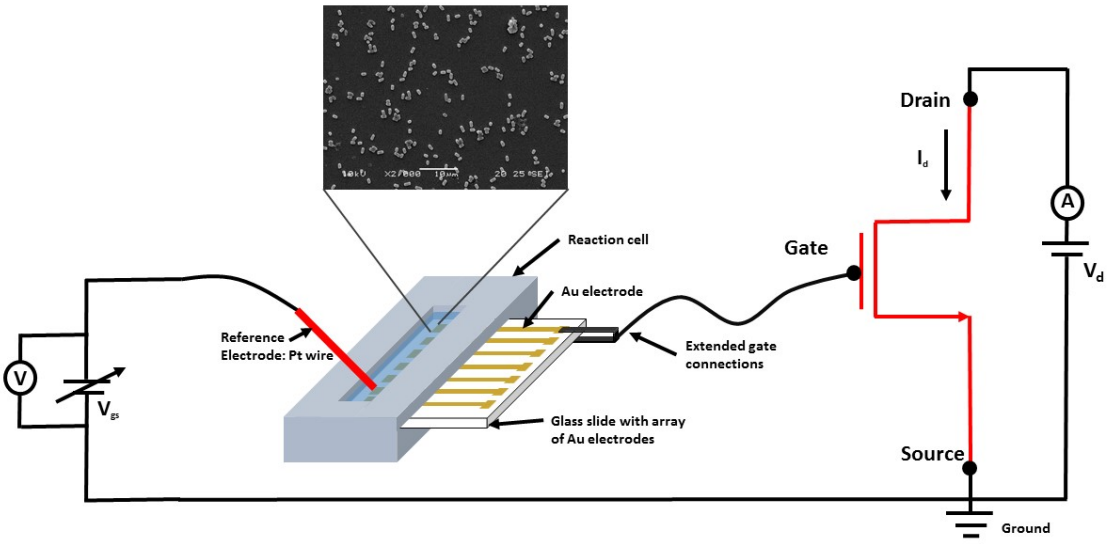

Figure1 - Working principle of the BioFET sensor. An array of evaporated gold electrodes placed in a flow cell is connected to the gate of a MOSFET. An external reference electrode is used to apply the gate voltage. The same electrodes were used for EIS and MALDI-ToF measurements.

3.1. Impedance

The bacterial detection was initially demonstrated by performing electrochemical impedance spectroscopy (EIS) capacitive measurements. The literature on capacitive sensors report both on positive (Carrara *et al.*, 2009; Varshney & Li, 2008; Couniot *et al.*, 2015a; Couniot *et al.*, 2015b) and negative changes in capacitance measurements (Webster *et al.*, 2009; Li *et al.*, 2011) after target binding. However, the behaviour of the sensor is dependent on the electrode type, immobilisation strategies, SAM properties and type of molecules detected. Ethylene-glycol terminated SAMs have hydrophilic properties (Carrara *et al.*, 2009; Ostuni *et al.*, 1999) that lead to the entrapment of water molecules within the SAM chains. For our sensor this phenomenon prevents the displacement of the ions in solution that form the Helmholtz plane upon bacteria binding. As a result, the bacteria and the underlying layers cannot be modelled simply by a series of capacitors (or as a single capacitor characterised by an increased distance separation d between the plates). Rather, the binding event will augment the surface of the electrode-solution interface which is surrounded by the solvent molecules forming the Helmholtz plane. Therefore, this can be modelled as two capacitors in parallel where the first has a fixed value and the value of the second capacitor is characterised by larger numbers of both d and relative permittivity ε_r (Asami *et al.*, 1980) and its extent

varies with the amount of bacteria bound onto the sugars on the gate of the BioFET. The combination of such factors following the bacterial adhesion to the glycosylated surface produce eventually a positive shift in the total capacitance. Exploiting the insulating properties of ethylene glycol-terminated SAMs (Carrara *et al.*, 2009; Berggren *et al.*, 2001), capacitive measurements are facilitated using non-Faradaic EIS.

A concentration of *Escherichia coli* PKL1162 equal to 4.2×10^9 CFU/mL produced an increase in the capacitance of $18.6 \pm 1.7\%$ (Figure 2). The EIS capacitance change decreased to $4.1 \pm 1.3\%$ when a decreased amount of 4.2×10^6 cell/mL of *Escherichia coli* PKL1162 were used as a target on mannose. The capacitance change follows approximately a Hill-type response of the form $y = y_{max}\, c^n/(k^n+c^n)$ where c is the concentration with y_{max}=22.8±1.4%, n=0.429±0.039, k=(1.37±0.47)×10^8 CFU/mL and a R^2 of 0.998 (although the small amount of data points needs to be taken into consideration when interpreting this R^2 value). Below 4.2×10^6 CFU/mL, the signal overlaps the values of capacitance change given by the negative control reactions, namely in presence of negative sugar probe (bacteria PKL1162 on GalNAc sugar), which produces a capacitance shift of $6.4 \pm 2.6\%$ and in presence of negative bacteria (K12 on mannose), which gives a capacitance change of $2.5 \pm 1.7\%$. Absolute values of capacitance range from 118 to 132 nF for electrodes functionalised with α-mannoside and from 123 to 155 nF upon bacterial adhesion.

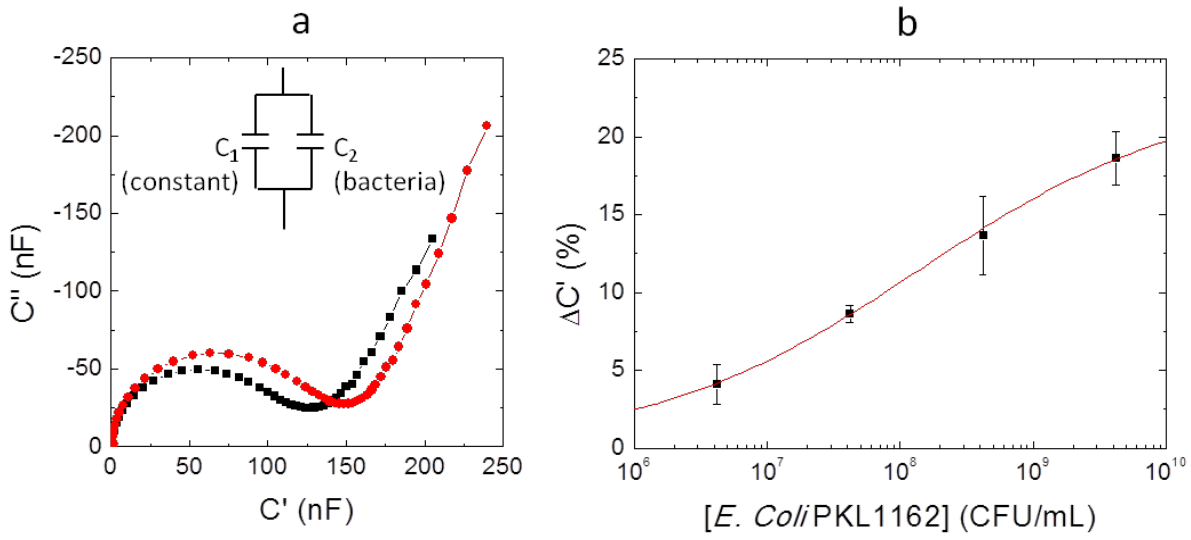

Figure 2 - Bacterial detection performing EIS capacitive measurements. a) Complex capacitance Cole-Cole plots for an electrode before (black line, squares) and after (red line, circles) *Escherichia coli* PKL1162 binding. The inset shows a schematic equivalent circuit.

b) Changes of the real part of the complex capacitance *vs.* bacterial concentration. The line represents a fit to the data with a Hill-type response (R^2= 0.998).

The use of a diluted measurement solution (PBS 1:100) reduced the ionic strength from 162 to 1.62 mM, which in turn, increased the Debye length from about 7.6 Å to 76 Å and improved the EIS detection by over five fold for the *Escherichia coli* PKL1162 concentration of 4.2×10^9 CFU/mL.

3.2. BioFET measurements

In the case of our BioFET, as in Figure 1, when the potential applied across the gate and the source (V_{gs}) is larger than the threshold voltage (V_{th}) of the device ($V_{gs}>V_{th}$), a conducting channel is formed between the source and the drain. Additionally, if a voltage is applied between the drain to source ($V_{ds}>0$) a current (I_D) begins to flow through the induced channel at the semiconductor. This condition of the device is known as the *turn-on* state where the electron-current (I_D) enters the drain and exits the source. Any changes in V_{gs} modulate the conductivity of the channel and thereby alter I_D. In the case of molecular interactions at the gate of the transistor, such as negatively charged *Escherichia coli* (Silhavy *et al.*, 2010) captured by surface mannosides, the minimum V_{gs} required to bring the n-MOSFET in the *turn-on* state is increased and it can be measured as an evidence of the binding event.

The negative charge of *Escherichia coli* produces a positive shift in the V_{gs} of the BioFET as can be seen in Figure 3a. Figure 3b presents the values of ΔV_{gs} for different bacteria concentration. ΔV_{gs} increases from 31.0 ± 11.9 mV to 115.2 ± 12.9 mV when the bacterial concentration increases from 1.9×10^5 CFU/mL to 4.2×10^9 CFU/mL. The voltage shift also follows a Hill-type response with y_{max}=150±23 mV, n=0.250±0.045, k=(4.26±6.03)×10^7 CFU/mL and a R^2 of 0.990. The lower value for 1.9×10^5 CFU/mL is still distinguishable from the signals obtained both in the presence of bacteria non-specific to the immobilised sugar ($\Delta V_{gs} = 8.7 \pm 1.3$ mV) and in the presence of a non-specific immobilised sugar ($\Delta V_{gs} = 16.2 \pm 1.5$ mV). BioFET measurements have the additional advantage of being very fast: data can be recorded in less than a second. Although EIS measurements could be recorded at a single frequency, which greatly shortens the time of the experiment as compared to the whole spectrum acquisition, miniaturisation of the devices would require long measurement sampling in order to accurately measure small a.c. current signals. On the

contrary, BioFETs are inherently miniaturisable as the shift of the threshold voltage is a charge density effect and hence the signal to noise ratio is preserved for miniaturised electrodes. The data presented demonstrates that BioFETs can be used for the initial differentiation between pathogenic and non-pathogenic *E. Coli* in order to decide which samples to send for further analysis.

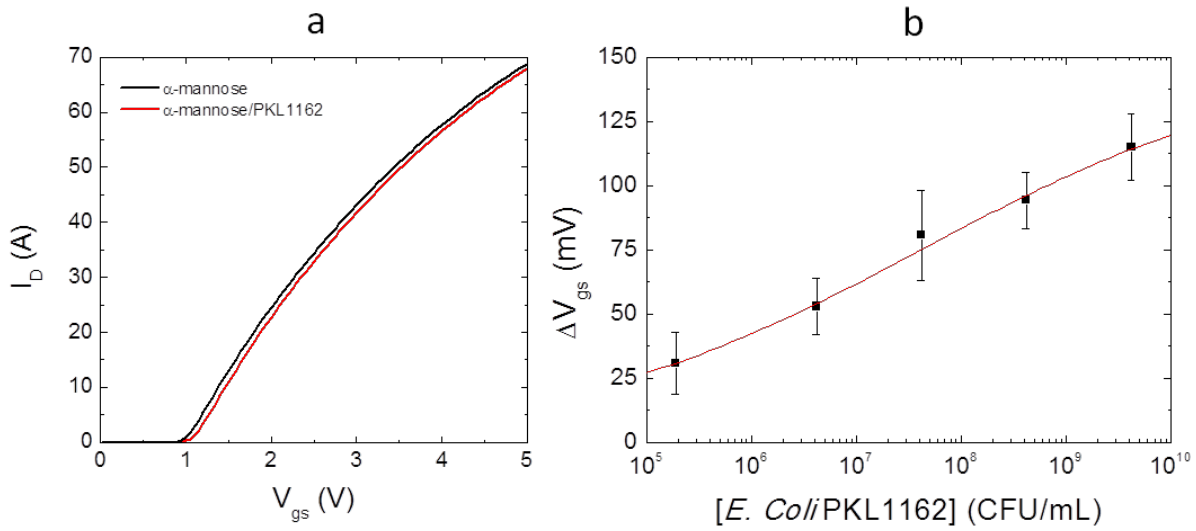

Figure 3 - Bacterial detection using BioFETs. a) BioFET I_D/V_{gs} characteristic for an electrode before (black line) and after (red line) *Escherichia coli* binding. b) V_{gs} changes *vs.* bacterial concentration. The line represents a fit to the data with a Hill-type response (R^2= 0.990). Error bars represent the standard deviation for three separate electrodes.

3.3. Scanning electron microscopy

Proof of bacterial binding and of good anti-fouling properties of the surface towards non-specific bacteria are confirmed by scanning electron microscopy (SEM). The SEM images in Figure 4 show surface bacterial coverage at different concentrations (from 4.2×10^9 to 4.2×10^5 CFU/mL) as well as in the presence of negative controls. The SEM pictures for negative controls are congruent with both the EIS and BioFET signals, even though BioFETs exhibited the highest sensitivity detecting much smaller amounts of PKL1162.

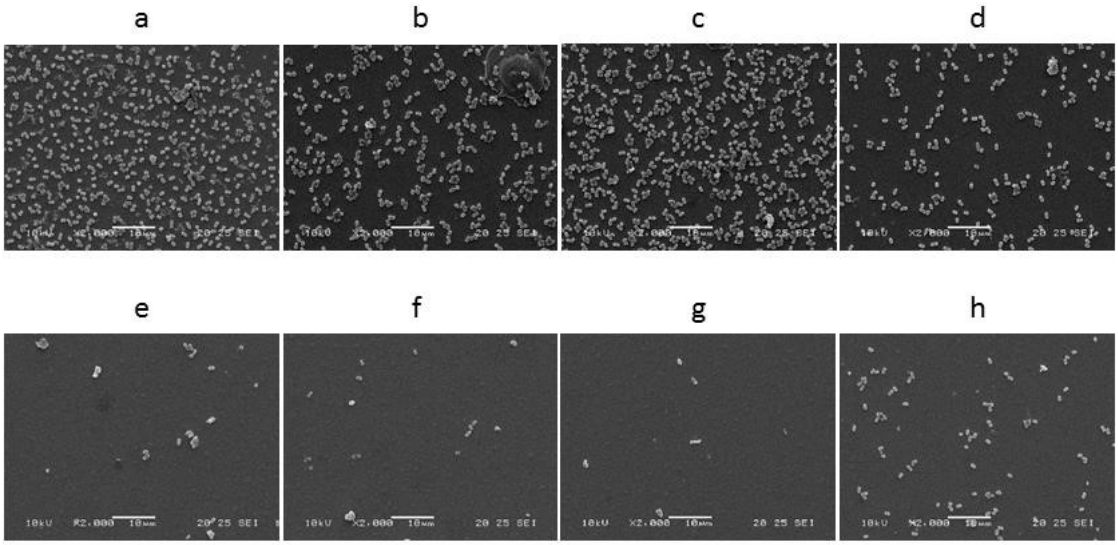

Figure 4 - SEM microscopy pictures of the affinity capture assay. Binding of *Escherichia coli* PKL1162 at the concentration of 4.2×10^9 (a), 4.2×10^8 (b), 4.2×10^7 (c), 4.2×10^6 (d), 4.2×10^5 (e), 4.2×10^4 (f), CFU/mL on α-mannose; *Escherichia coli* strain K12 at the concentration of 4.2×10^9 on α-mannose (g) and *Escherichia coli* strain PKL12 at the concentration of 4.2×10^9 on GalNAc (h).

3.4. MALDI-ToF mass spectrometry

Glycan functionalisation of SAMs was confirmed using MALDI- ToF MS on both gold arrays and on gold arrays evaporated on glass by direct surface ionisation (see Supplementary Information). Specific peaks situated at 12000 and 16000 m/z corresponding to MS fingerprint of *Escherichia coli* PKL1162 can be observed by performing MS on bacterial sample spotted on bare gold without SAM functionalisation (Figure 5a-Control). Such peaks were also detected in the affinity reaction not only when performing the measurements on gold arrays but also on the gold arrays evaporated on glass as it can be seen in Figure 5a. The specificity of α-D-mannose towards *Escherichia coli* strain PKL1162 is shown in the Supplementary Information where *Escherichia coli* PKL1162 peaks are only clearly visible after affinity capture and washing, when the gold electrodes are functionalised with α-D-mannose but not with other sugars. Moreover, although SEM microscopy shows significant bacterial adhesion using samples of *Escherichia coli* PKL1162 diluted up to 4.2×10^6 CFU/mL (Figure 4), a minimum concentration of 2.7×10^9 CFU/mL was required to produce observable peaks using MALDI-ToF on gold plate (Figure 5b). MALDI-ToF spectra

also showed absence of any significant non-specific attachment of *Escherichia coli* K12 on α-mannose (Figure 5b, bottom image) as well as on other sugars (Supplementary Information).

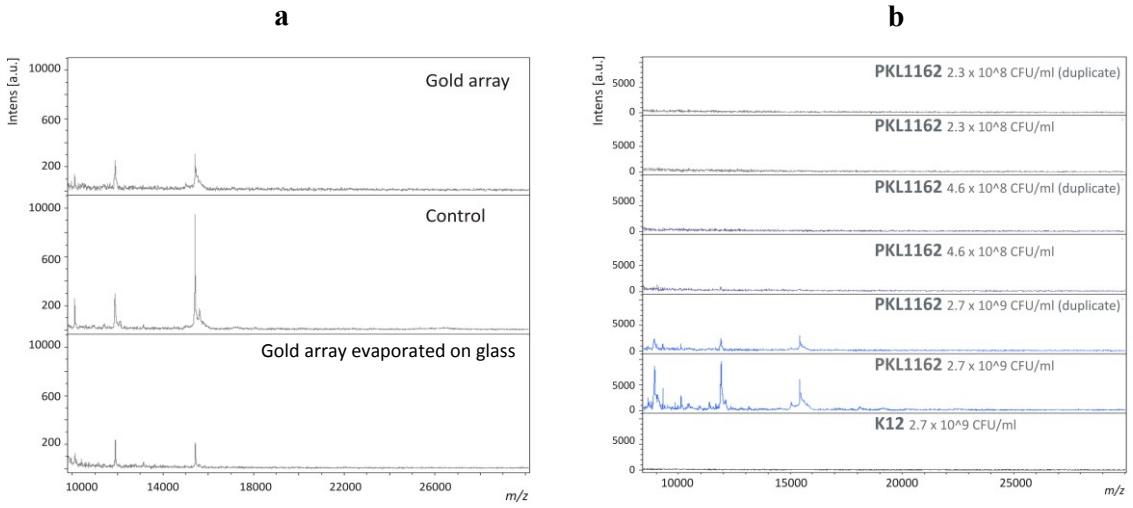

Figure 5 - MALDI-ToF spectra of the affinity capture assay. a) MALDI-ToF spectra of uropathogenic *Escherichia coli* PKL1162 after affinity capture on α-D-mannose covalently linked to gold electrodes evaporated on glass slides (top image), of *Escherichia coli* PKL1162 spotted on bare gold (middle plot) and *Escherichia coli* PKL1162 after affinity capture on α-D-mannose covalently linked to gold arrays (bottom image). The peaks at12000 and 16000 m/z are diagnostic for *Escherichia coli* PKL1162. b) MALDI-ToF spectra responses for different concentrations of *Escherichia coli* PKL1162 on α-D-mannose. The analysis was performed on SAM-functionalised gold plates, *Escherichia coli* K12 was used as negative control and showed no peaks upon MS analysis.

In Table 1 the *time of measurements* and the *limit of quantitation* (LOQ) of our BioFET are compared to the ones obtained by our EIS and MALDI-ToF measurements and show a significant improvement (over 100 fold) of readout time. In the EIS set up, the absence of redox molecules simplified the assay with respect to conventional Faradaic EIS experiments. However, the EIS signal is a resultant of combined – and often competing – effects of the variation of surface area coverage, relative permittivity and the distance between the electrode and the Helmholtz plane upon bacterial binding, which can hinder the detection of low levels of bacteria.

Table 1. BioFET, MALDI-ToF MS and EIS are compared in terms of limits of quantitation (LOQ) and time for carrying out the measurements in this work. The comparison is obtained considering that the three techniques were used on the same electrodes. Therefore, immobilisation times of the electrodes as well as the bacterial growth are not considered as they are equal for all the assays here reported.

Technique	LOQ (CFU/mL)	Time required for the measurement
BioFET	1.9×10^5	~ 2 s
EIS	4.2×10^7	~ 10 min
MALDI-ToF MS	2.7×10^9	~ 20 min

These effects are not as significant in the case of BioFETs. Using the electrodes as extended gates for MOSFETs, the sensor response is mostly due to the bacterial charge, thereby resulting in an LOQ being improved by more than two orders of magnitude (Table 1).

With respect to MS detection, the sensitivity of the BioFETs is four orders of magnitude greater, which, together with its significantly reduced cost when compared to a MALDI-ToF instrument (considering a similar price for the sensor array), confirms the value of our sensor. Although low limits of bacteria detection have been reported for other types of biosensors (Ahmed *et al.*, 2014), the mass-production of MOSFETs and the ease of integration into multiplexed devices with commercial planar processes for large-scale circuitry using standard semiconductor technologies such as CMOS, which has already been widely demonstrated by their ubiquitous use in everyday applications, can allow multiple screening of samples without leading to a significant increase in the costs of the sensor. Each individual multiplexed chip can be mass produced at very low cost (typically below $1) and the use of glycosides instead of *e.g.* antibodies as recognition elements doesn't had significant costs to the biochips. Furthermore, the readout system is straightforward from an electronics point of view and can be produced at a fairly low cost (below $100). Obviously the fingerprint given by techniques such as MALDI-ToF or PCR is essential for obtaining detailed information such as antimicrobial susceptibility, virulence and intra-species typing (Didelot *et al.*, 2012; Formisano *et al.*, 2015). However, such evidence is only needed once the pathogenicity of a sample has been confirmed. The ability to use an initial low-cost screening to limit the need

for more accurate and expensive techniques would significantly optimise times and costs of the examinations.

4. Conclusions

With the BioFET sensor developed in this work we have specifically detected uropathogenic *Escherichia coli* strains expressing type 1 fimbriae, which are responsible for the great majority of urinary tract infections (Ronald, 2003). The FimH protein on the type 1 fimbriae binds to the α-D-linked mannoses on glycoproteins of urinary epithelial cells. The BioFET sensors are highly applicable for bacteria-glycan interactions by using other glycans as targets for protein recognition; for example terminal sialic acid on gastrointestinal human mucins can be recognised by *H. pylori* SabA adhesin (Mahdavi *et al.*, 2002) while *Vibrio cholerae* GbpA ahesin mainly binds to GalNAc (Bhowmick *et al.*, 2008).

Upon the binding of bacteria to functionalised electrodes, charges at the membrane of the bacteria and the displacement of water and ions from the biolayer surface (due to the presence of the large bacteria), disturbs significantly the electrochemical double layer capacitance. This in turn causes a shift on the threshold potential of the BioFETs. The BioFET will provide a signal to any type of bacteria that binds to the functionalised electrodes. For example, in Gram-positive bacteria the negative charge is mostly due to the presence of negatively charged phosphate in teichoic acids – teichoic acids are linked to either the peptidoglycan or to the underlying plasma membrane. For Gram-negative bacteria, the outer bacterial wall is covered by phospholipids and lipopolysaccharides and the charge is mostly given by the strong negative charge of lipopolysaccharides. Furthermore all bacteria will cause displacement of water ions from the biolayer further changing the electrochemical double layer capacitance.

In conclusion we have demonstrated a fast, effective and inexpensive sensor that can be used to support current clinical microbiology by providing high-throughput screening of pathogenic bacterial samples. Our technology can be easily implemented and would be performed after the enrichment step and before further advanced investigations so that additional time and costs can be saved in the area of traditional bacterial detection. The results show through the use of suitable molecular probes, the BioFETs can differentiate pathogens that can be used for multiplexed screening. The large volume production of such

chips will bring the assay price further down, making it an attractive proposition for pathogen screening in point of care applications.

Acknowledgments

The authors thank Dr Susana Liébana Girona for important discussions. This work was partly funded by the European Union's Seventh Framework Programme for research, technological development and demonstration under grant agreement no. 278832 (hiPAD, 2012-2016), 259869 (GlycoBioM, 2012-2015) and 317420 (PROSENSE, 2012-2016). JRM thanks CONACyT for a doctoral scholarship.

References

Ahmed, A., Rushworth, J., Hirst, N. & Millner, P. Biosensors for whole-cell bacterial detection. *Clin. Microbiol. Rev.* **27,** 631-646 (2014).

Asami, K., Hanai, T. & Koizumi, N. Dielectric analysis of Escherichia coli suspensions in the light of the theory of interfacial polarization. *Biophys. J.* **31,** 215-228 (1980).

Berggren, C., Bjarnason, B. & Johansson, G. Capacitive biosensors. *Electroanalysis* **13,** 173-180 (2001).

Bhowmick *et al.* Intestinal adherence of *Vibrio cholera* involves a coordinated interaction between colonization factor GbpA and mucin. *Infect. Immun.* **76**, 4968-4977 (2008).

Both, P. *et al.* Discrimination of epimeric glycans and glycopeptides using IM-MS and its potential for carbohydrate sequencing. *Nat. Chem.* **6,** 65-74 (2014).

Brachman, P. & Abrutyn, E. *Bacterial Infections of Humans*. (Springer Science+Business Media, 2009).

Carrara, S. *et al.* Label-free cancer markers detection by capacitance biochip. *Sens. Actuators B* **136,** 163-172 (2009).

Coates, A., Hu, Y., Bax, R. & Page, C. The future challenges facing the development of new antimicrobial drugs. *Nat. Rev. Drug Discov.* **1,** 895-910 (2002).

Couniot, N., Afzalian, A., Van Overstraeten-Schlögel, N., Francis, L. & Flandre, D. Capacitive biosensing of bacterial cells: analytical model and numerical simulations. *Sens. Actuators B* **211,** 428-438 (2015a).

Couniot, N. *et al.* Lytic enzymes as selectivity means for label-free, microfluidic and impedimetric detection of whole-cell bacteria using ALD-Al_2O_3 passivated microelectrodes. *Biosens. Bioelectron.* **67,** 154-161 (2015b).

Didelot, X., Bowden, R., Wilson, D., Peto, T. & Crook, D. Transforming clinical microbiology with bacterial genome sequencing. *Nat. Rev. Genet.* 13, 601-612 (2012).

Estrela, P. *et al.* Label-Free Sub-picomolar protein detection with field-effect transistors. *Anal. Chem.* **82,** 3531-3536 (2010).

Estrela, P., Stewart, A., Yan, F. & Migliorato, P. Field effect detection of biomolecular interactions. *Electrochim. Acta* **50,** 4995-5000 (2005).

Formisano, N. *et al.* Multimodal electrochemical and nanoplasmonic biosensors using ferrocene-crowned nanoparticles for kinase drug discovery applications. *Electrochem. Commun.* **57,** 70-73 (2015).

Fournier, P.E. *et al.* Modern clinical microbiology: new challenges and solutions. *Nat. Rev. Microbiol.* **11**, 574-585 (2013).

Foxman, B., Barlow, R., D'Arcy, H., Gillespie, B. & Sobel, J.D. Urinary tract infection: self-reported incidence and associated costs. *Ann. Epidemiol.* **10**, 509-515 (2000).

Hartmann, M. & Lindhorst, T. The bacterial lectin FimH, a target for drug discovery - carbohydrate inhibitors of type 1 fimbriae-mediated bacterial adhesion. *Eur. J. Org. Chem.* **2011,** 3583-3609 (2011).

Kang, D. *et al.* Rapid detection of single bacteria in unprocessed blood using integrated comprehensive droplet digital detection. *Nat. Commun.* **5,** 5427 (2014).

Li, D. *et al.* Label-free capacitive immunosensor based on quartz crystal Au electrode for rapid and sensitive detection of Escherichia coli O157:H7. *Anal. Chim. Acta* **687,** 89-96 (2011).

Ma, F. *et al.* Glycosylation of quinone-fused polythiophene for reagentless and label-free detection of E. coli. *Anal. Chem.* **87,** 1560-1568 (2015).

Mahdavi *et al. Helicobacter pylori*SabA adhesion in persistent infection and chronic inflammation. *Science* **297**, 573-578 (2002).

Mannoor, M. *et al.* Graphene-based wireless bacteria detection on tooth enamel. *Nat. Commun.* **3,** 763 (2012).

Mohanty, N. & Berry, V. Graphene-based single-bacterium resolution biodevice and DNA transistor: interfacing graphene derivatives with nanoscale and microscale biocomponents. *Nano Lett.* **8,** 4469-4476 (2008).

Noble, G. *et al.* Accelerated enzymatic galactosylation of N -acetylglucosaminolipids in lipid microdomains. *J. Am. Chem. Soc.* **134,** 13010-13017 (2012).

Oelschlaeger, T., Dobrindt, U. & Hacker, J. Virulence factors of uropathogens. *Curr. Opin. Urol.* **12,** 33-38 (2002).

Ostuni, E., Yan, L. & Whitesides, G. The interaction of proteins and cells with self-assembled monolayers of alkanethiolates on gold and silver. *Colloids Surf. B* **15,** 3-30 (1999).

Poghossian, A. & Schöning, M.J. Label-free sensing of biomolecules with field-effect devices for clinical applications. *Electroanalysis* **26**, 1197-1213 (2014).

Reisner, A., Haagensen, J., Schembri, M., Zechner, E. & Molin, S. Development and maturation of Escherichia coli K-12 biofilms. *Mol. Microbiol.* **48,** 933-946 (2003).

Ronald, A. The etiology of urinary tract infections: traditional and emerging pathogens. *Dis. Mon.* **49**, 71-82 (2003).

Šardzík, R. *et al.* Preparation of aminoethyl glycosides for glycoconjugation. *Belstein J. Org. Chem.* **6,** 699-703 (2010).

Šardzík, R. *et al.* Chemoenzymatic synthesis of O-mannosylpeptides in solution and on solid phase. *J. Am. Chem. Soc.* **134,** 4521-4524 (2012).

Silhavy, T., Kahne, D. & Walker, S. The bacterial cell envelope. *Cold Spring Harb. Perspect. Biol.* **2,** a000414-a000414 (2010).

Stein, R. Super-spreaders in infectious diseases. *Int. J. Infect. Dis.* **15,** e510-e513 (2011).

Varshney, M. & Li, Y. Double interdigitated array microelectrode-based impedance biosensor for detection of viable Escherichia coli O157:H7 in growth medium. *Talanta* **74,** 518-525 (2008).

Webster, M., Timoshkin, I., Macgregor, S. & Mattey, M. Computer aided modelling of an interdigitated microelectrode array impedance biosensor for the detection of bacteria. *IEEE Trans. Dielectr. Electr. Insul.* **16,** 1356-1363 (2009).

Weissenborn, M. *et al.* Formation of carbohydrate-functionalised polystyrene and glass slides and their analysis by MALDI-TOF MS. *Beilstein J. Org. Chem.* **8,** 753-762 (2012).

Zhi, Z. *et al.* A versatile gold surface approach for fabrication and interrogation of glycoarrays. *ChemBioChem* **9,** 1568-1575 (2008).

Zourob, M., Elwary, S. & Turner, A. *Principles of Bacterial Detection*. (Springer, 2008).